PHASE INSTABILITY IN HASTELLOY N

R. E. Gehlbach and H. E. McCoy, Jr.*

ABSTRACT

Though Hastelloy N is basically a solid-solution alloy, various thermomechanical treatments do change its mechanical properties and microstructure. Since it is intended for use up to 850°C and is now used in molten fluoride salt reactor systems, we must understand the nature of the precipitation processes and the effect on mechanical behavior.

Identifying and characterizing the precipitates involved several complementary techniques: optical metallography, transmission electron microscopy, extraction replication, x-ray diffraction, and electron probe microanalysis. In addition, chemical analysis with a microprobe attachment for the electron microscope and electron diffraction were employed to identify individual particles, agglomerates, and grain-boundary films on extraction replicas without interference from the matrix. These techniques help resolve differences in precipitates and relate the microstructure to mechanical properties.

The microstructure is characterized by stringers of massive primary precipitates of the Ni_3Mo_3C type. Exposure between 500 and 1000°C results in precipitation of particles of the Ni_2Mo_4C type in the grain boundaries. In air-melted heats that contain approximately 0.6% Si, the carbide-type precipitates are enriched in silicon and are not dissolved at high annealing temperatures but melt and transform to a noncarbide phase. In vacuum-melted heats with low silicon contents, carbides go into solid solution.

The only precipitates that form in air-melted alloys at temperatures as high as 1180°C are complex pseudocarbides of the $Ni_3(Mo,Cr)_3(C,Si)$ and $Ni_2(Mo,Cr)_4(C,Si)$ types. The amount and behavior of precipitates are highly silicon dependent; this impurity stabilizes the particles, preventing their being taken into solid solution at high annealing temperatures and causing them to transform to the high-temperature phase. This latter phase is possibly the δ-NiMo intermetallic and is probably responsible for the increased embrittlement at high annealing temperatures.

---

*Metals and Ceramics Division, Oak Ridge National Laboratory, operated by Union Carbide Corporation for the U.S. Atomic Energy Commission.

INTRODUCTION

We have studied Hastelloy N, an alloy developed at Oak Ridge National Laboratory (ORNL) specifically for use with molten fluoride salts. (1) It is nickel-base, solid-solution strengthened with 16% Mo, and contains 7% Cr for moderate oxidation resistance. It also contains several other elements with the exact concentrations depending somewhat upon the melting practice. The specified chemical composition of Hastelloy N and typical compositions of air- and vacuum-melted heats are given in Table 1. Our studies show that one of the most important elements in controlling the precipitation is silicon, which is much lower in the vacuum-melted than in the air-melted material.

Since this alloy is used routinely in the temperature range of 600 to 800°C, we are concerned with how the mechanical properties change over long periods of time. Although Hastelloy N is basically a solid-solution-strengthened alloy and does not exhibit classical age hardening, the mechanical properties (particularly the fracture strain) can be altered markedly by various thermal and mechanical treatments.

The primary goal of our work has been to relate microstructure to mechanical behavior. We have found that this is an extremely complicated problem and that it requires the use of many experimental tools including conventional metallography, electron microprobe analysis, transmission electron microscopy, electron and x-ray diffraction, extraction replication, and autoradiography. Because of the complexity of the problem, we have not completely satisfied our goal of having a one-to-one correlation between microstructure and properties. However, our findings to date are very informative and, in many cases, quite unexpected.

EXPERIMENTAL TECHNIQUES

The mechanical properties of Hastelloy N as a function of thermal and mechanical treatments were determined under tensile and creep conditions, at test temperatures ranging from ambient to nearly 1000°C. Some of the tensile tests were run in a hydraulic Baldwin testing machine at a strain rate of approximately 0.025 min^{-1} and others were run in a mechanically driven Instron Universal Testing machine where the strain rate could be controlled over the range of 2 to 0.002 min^{-1}. A standard equilibrating time of 1/2 hr was used before each tensile test to allow the specimen sufficient time to reach temperature. All tests were run in an air environment.

All heat treatments prior to testing were carried out in an argon atmosphere. The specimens were cooled from the annealing temperature by pulling them from the hot zone into the water-cooled end of the furnace tube. The average cooling rate down to 300°C was about 300°C/min.

Metallographic examination was routinely used for evaluation of precipitation, grain structure, and fracture mode. We selected certain specimens for more intensive study by a variety of complementary techniques. Transmission electron microscopy specimens were prepared from bulk material, usually slices cut from tensile specimens or heat-treated rod. Our specimen preparation technique (2) consists of initially dimpling 20-mil slices which are subsequently electropolished.

To examine and analyze the various morphologies present in the material, we prepared direct carbon electrolytic extraction replicas using a 10% HCl—ethyl alcohol electrolyte.

Phase analysis was performed primarily by electron and x-ray diffraction and microprobe techniques. Grain boundary precipitates on the extraction replicas were usually thin enough to provide good electron diffraction patterns. Large precipitates were frequently sufficiently thin at the edges that patterns could be obtained from them, particularly in transmission specimens. X-ray diffraction analysis was carried out both on extraction replicas and bulk electrolytic extraction residues.

Chemical analysis involved the use of a conventional electron microprobe and also an electron microprobe accessory for one of our electron microscopes. The former was used for analyses of large precipitates, matrix material and areas of heavy fine precipitation. Grain boundary precipitates were much too fine for analysis using conventional techniques and matrix dilution effects prevented analysis of small precipitates. The microanalyzer accessory for the electron microscope has provided us with a tool for analyses of fine precipitates and grain boundary films on extraction replicas.

We have also used autoradiographic techniques to follow carbon-14, which was introduced into a melt of Hastelloy N. Liquid emulsions (Kodak NTB-2 and NTE) were spread over the surface of metallographic specimens and developed and photographed *in situ* following appropriate exposure times. By this method, the distribution of carbon could be determined with the subsequent identification of carbon and noncarbon phases.

EXPERIMENTAL RESULTS

Hastelloy N exhibits a considerable loss in elevated temperature ductility following annealing treatments although changes in strength are not nearly so pronounced. (3) Figure 1 shows the variation in ductility with test temperature in air-melted Hastelloy N for two pretest annealing temperatures. The ductility minimum at elevated temperatures has been shown to be typical of many metals and alloys. (4) We found for Hastelloy N that increasing the pretest annealing temperature decreased the minimum ductility and increased the temperature at which the minimum occurred. The temperature of the ductility minimum after annealing at 1177°C varied slightly from heat to heat and with strain rate covering the temperature range of about 650 to 900°C. We measured the variation of the minimum ductility with pretest annealing temperature for a heat of material that had its minimum ductility at about 870°C. As shown in Fig. 2, the ductility decreases as the material is annealed above the recommended temperature of 1180°C.

Microstructural Observations

The microstructure of Hastelloy N is characterized by large precipitates formed during casting which remain after annealing, as shown in Fig. 3. They are heterogeneously distributed in stringers along the direction of fabrication. The grain size varies widely as a function of these large particles, identified as M_6C-type carbides by x-ray and electron diffraction with a lattice parameter of about 11.02 A.

The fracture process at temperatures below 600°C is transgranular and the large carbide-type particles readily crack, offering a profuse supply of cracks, as shown in Fig. 4a. Figure 4b shows the typical intergranular separation and recrystallization found in specimens tested at 980°C following a pretest anneal of 1180°C. A pretest anneal at 1260°C results in intergranular failure without extensive cracking away from the fracture and without recrystallization (Fig. 4c). At elevated test temperatures, few cracked particles are found but a considerable amount of grain boundary precipitation is produced.

A tensile prestrain at room temperature following a 1260°C anneal greatly improves the ductility at 870°C. Since the large particles are cracked by the prestrain, this suggests that crack nucleation is not a controlling factor in the elevated temperature embrittlement but that an embrittling grain boundary phase present after the anneal could be important. Grain boundaries etch much more readily following a

1260°C anneal than after an 1180°C anneal, further suggesting the formation of a grain boundary film during the higher temperature anneal.

Grain boundary precipitation occurs on a relatively fine scale for short exposures to temperatures in the range of 500 to 700°C. On increasing time at these lower temperatures, the precipitates, originally in a fine dendritic morphology, coarsen and agglomerate. At higher aging temperatures, the precipitation is much more extensive and covers large grain boundary areas, often as massive sheets or cellular morphologies. An exception to the above observation is found in material fractured at high temperatures where the ductility is recovered (see Fig. 1). In this case, the alloy has recrystallized and the grain boundaries are free of precipitate. The various grain boundary morphologies on extraction replicas appear to have the same crystallography as the blocky M_6C-type precipitates with a lattice parameter of about 11.02 A, determined by x-ray and electron diffraction. X-ray diffraction from bulk extraction residues containing both the primary and grain boundary precipitates shows only the single parameter. Table 2 lists the intensities from these precipitates.

Precipitate Analysis

Analysis of the large carbides in the bulk material by conventional microprobe techniques reveals that they are quite complex and contain about 34% Ni, 55% Mo, 5% Cr, 2.5% Si, 1.7% or more C, plus minor amounts of iron and manganese. Although the nominal molybdenum concentration in the alloy is 16%, microprobe analysis shows that only 12% is present in the matrix. The matrix also exhibits a considerable depletion of silicon containing about 0.3% rather than the 0.6% present in the bulk alloy.

Figure 5 is an extraction replica from Hastelloy N aged 4 hr at 870°C following an 1180°C anneal. The dendritic precipitate has essentially the same lattice parameter as the blocky M_6C-type particles as mentioned earlier. Both the large blocky and dendritic M_6C-type carbides in this extraction were analyzed using the electron microscope microprobe accessory. The results for the blocky particles are in excellent agreement with results from the conventional microprobe. These precipitates are close to the stoichiometric Ni_3Mo_3C, which would contain 37, 60.5, and 2.5% Ni, Mo, and C, respectively, with the chromium substituting for part of the molybdenum. The dendritic precipitates are found to contain approximately 15–20% Ni, 70–75% Mo, 2–4% Cr, and 2.5–4.5% Si. The microprobe accessory is not equipped for carbon analysis and since these precipitates are much too fine to be resolved in the conventional microprobe, a carbon determination

for the grain boundary phase is not possible. The composition of the dendritic morphology is similar to a Ni_2Mo_4C-type stoichiometry, which would have 22.9, 74.8, and 2.3% Ni, Mo, and C, respectively.

We confirmed the identity of these precipitates as carbides by autoradiography, using carbon-14 as the tracer radioisotope. Figure 6 shows the microstructure of this alloy, annealed at 1177°C and aged 100 hr at 650°C, without and with the photographic emulsion on the specimen. It is seen that areas of increased activity (dark regions) exist at particles and in the grain boundaries.

When commercial air-melted Hastelloy N is exposed to temperatures in excess of 1300°C, as encountered in welding, the large precipitates do not go into solution but transform to a lamellar-like product or a massive grain boundary phase. In contrast, evaluation of a commercial vacuum-melted heat revealed that the carbides do go into solution and that the high-temperature phase does not form. These conditions are shown in Fig. 7. The major compositional difference between the air- and vacuum-melted alloys is the concentration of silicon, which was added to deoxidize the air melts. X-ray diffraction studies of extraction residue show the presence of two phases in this material aged 1 hr at 870°C following an anneal at 1260°C.

The stringered precipitates, M_6C, were present and, in addition, Mo_2C was a strong phase. About 10%, by weight, of the molybdenum in this carbide was replaced by chromium and the lattice constants, contracted slightly from the reported values of hexagonal Mo_2C, of $a = 2.98$ Å and $c = 4.688$ Å were determined. The strongest lines are listed in Table 2.

Effect of Composition on Precipitation

The effect of molybdenum concentration on precipitation was evaluated since microprobe analysis indicated that only 12% was present in the bulk alloy. Several laboratory melts containing the nominal 7% Cr, 4% Fe, and 0.06% C with 10, 12, 16, and 20% Mo were prepared. Figure 8 shows that the precipitates were present only when the molybdenum concentration was above 12%. X-ray diffraction of extraction residues from an alloy containing 12% Mo, 7% Cr, 4% Fe, 0.06% C, and 0.5% Si reveals that Mo_2C is again present as a strong phase, in addition to the M_6C-type carbides. Exposure of this material to very high annealing temperatures results in the formation of the high-temperature grain boundary and lamellar phases, as seen in Fig. 9.

Therefore, high levels of molybdenum and silicon both tend to stabilize M_6C carbide-type precipitation whereas Mo_2C is promoted when either of these elements are present in concentrations of 12% and trace levels, respectively. It appears that silicon is responsible for causing the primary M_6C-type particles to transform to the high-temperature phase rather than dissolve at high annealing temperatures.

To evaluate more fully the possible effects of silicon on the precipitate behavior, a series of alloys of nominal composition (16% Mo, 7% Cr, 4% Fe, and 0.06% C) with silicon concentrations ranging from 0.02 to 1.05% were prepared. Figure 10 shows that the amount of precipitate increases with increasing silicon. The as-cast structure is retained somewhat in the alloy containing 0.48% Si, and to a great extent in the alloy containing 1.05% Si after annealing at 1180 and 1260°C. The concentration of silicon in the precipitates present after casting or low-temperature anneals, as determined by conventional microprobe analysis, increases with increasing total silicon content of the alloy. The analyses were hindered because of the small precipitate size, but a large beam size used to cover a field composed of many particles resulted in these areas being two to five times richer in silicon than the total alloy concentration. The matrix composition was found to be approximately one-half the total silicon concentration in the alloy.

We made extraction replicas from the 1.05% Si alloy after annealing at 1260°C. The grain boundaries were nearly continuously covered by thin precipitate films and associated with particles in the grain boundaries. Microprobe analyses of the particles and films using the electron microscope accessory indicated compositions similar to those found in the commercial alloys but enriched in silicon to nearly 5%. Electron and x-ray diffraction patterns failed to show any change in lattice parameters from the usual 11 A.

On the other hand, these precipitates behave quite differently at high annealing temperatures, as seen in Fig. 11. At low silicon levels, the precipitates go into solution and grain growth results whereas grain boundary melting and high-temperature phase formation occur at the higher silicon levels, indicating that this transformation product is dependent on the silicon concentration. We found that the temperature for this transformation was lower for the alloy containing 1.05% Si than for the 0.48% Si alloy.

We have also found that the high-temperature phase is present in the heat-affected zone of welded material. The blocky carbides transform into the lamellar high-temperature phase near the fusion line. Microprobe analysis shows that areas containing this lamellar phase in the commercial air-melted alloy are enriched in silicon, further supporting the association of silicon with the phase transformation.

X-ray diffraction patterns of extractions from material annealed at 1370°C to give the high-temperature phase fail to show any lines different from those of the usual M_6C. Analysis of the phase on extraction replicas taken from a lightly etched specimen resulted in a lattice parameter of 11.0 A, determined by electron diffraction, and the Ni_2Mo_4C-type composition. However, the precipitate present on the replica was quite thin and its appearance, as shown in Fig. 12, indicated attack by the electrolyte.

We subsequently prepared an extraction replica from the fracture surface of a specimen of air-melted stock which had been annealed at 1260°C and fractured at 870°C in argon. The fracture surface contained a large amount of various morphologies of precipitate of the M_6C type, as shown in Fig. 13, indicating that the grain boundary precipitate may be responsible for the reduction in the high-temperature ductility after annealing at 1260°C (Fig. 1). It is seen that one morphology has definitely been attacked by the electrolyte.

Autoradiography carried out on a specimen containing carbon-14 clearly shows that carbon is rejected from the high-temperature phase suggesting that this lamellar product is a transformation from a carbide to a noncarbide, as shown in Fig. 14. All activity from the carbon-14 emanates from the matrix adjacent to the lamellae.

We have obtained very weak diffraction lines in addition to matrix and M_6C, from a polished metallographic specimen containing the high-temperature phase. Some M_6C is present but additional lines closely fit those reported by Guthrie and Stansbury *et al.* (5) and Shoemaker *et al.* (6) for the delta, or NiMo intermetallic phase. Electron diffraction patterns from thin areas in this phase present in transmission specimens give d-values quite similar to those for this intermetallic phase. (6) The structure of this phase is complex with many possible lines, making identification by electron diffraction difficult. However, the d-values can be accounted for with the delta nickel-molybdenum phase.

DISCUSSION

In general, we have observed that the microstructure of Hastelloy N contains blocky, primary precipitates of the M_6C type which are stable to temperatures slightly higher than the 1180°C recommended annealing temperature, both in air- and vacuum-melted heats. On exposure to temperatures in the range of 400 to 1000°C, the air-melted heats exhibit profuse grain boundary precipitation of M_6C-type particles in various morphologies. In the vacuum-melted material, however, $(Mo,Cr)_2C$ carbides are present in large quantities. The only significant difference in composition between the several air- and vacuum-melted heats is in the concentration of silicon, added to the former as a deoxidizer.

Analyses of the M_6C-type particles in the air-melted material indicate that the blocky, or stringered, primary precipitates are close to the Ni_3Mo_3C type and that the grain boundary morphologies are similar in composition to a Ni_2Mo_4C type. Both types are quite complex, contain appreciable amounts of chromium, and are enriched in silicon to a level of 2–4% by weight.

The most striking contrast between the air- and vacuum-melted alloys is evidenced after exposure to high annealing temperatures. The M_6C carbides in the vacuum-melted low silicon material are put into solid solution whereas in the alloys bearing higher silicon, the precipitates transform to a complex noncarbide phase, and in many cases, grain boundary melting occurs. Small laboratory heats containing various levels of silicon confirm that this element is responsible for the high-temperature phase. The transformation appears to be quite complex and analyses are not yet sufficiently clear to allow us to specifically identify the phase. We have strong evidence based on electron and x-ray diffraction that the phase is the δ-NiMo intermetallic. It appears reasonable that the 1:1 intermetallic could result from a decomposition of a Ni_3Mo_3C- or a Ni_2Mo_4C-type particle, particularly when the latter is adjacent to a nickel-rich matrix. It also is seen that this intermetallic melts in the nickel-molybdenum system at 1350°C, the approximate temperature where localized melting of the high-temperature phase in Hastelloy N is observed. Furthermore, we found that increased amounts of silicon lowered the temperature at which the M_6C-type precipitates would melt and/or transform. It is reasonable, then, that the silicon stabilizes and promotes the formation of the intermetallic phase.

Both metallographic and electron microprobe analyses have shown that the solid solubility of molybdenum in Hastelloy N is approximately 12%. Since the total concentration in the alloy is approximately 16%, it is apparent that in the air-melted material (containing only M_6C-type precipitates), 4% Mo must be tied up in the precipitates. The primary

particles (Ni_3Mo_3C-type) comprise the major portion of precipitate. If we would assume that 80% of the total 0.06% C is tied up as Ni_3Mo_3C with the remainder as Ni_2Mo_4C, the total carbon could accommodate only 1.2 and 0.4% Mo, respectively, far from the 4% which must be accounted for. Actually, the chromium is expected to replace a portion of the molybdenum, which would lower these values. The precipitates are enriched in silicon and the silicon concentration in the matrix is roughly 0.3% for an alloy containing approximately 0.6% in the bulk. If we assume that the silicon may replace carbon in the M_6C-type structure and calculate the amount of molybdenum tied up by 0.06% C and 0.3% Si, the resultant matrix would contain approximately 12% Mo, in agreement with experimental evidence.

Our findings, then, indicate that the phase instability in Hastelloy N results from silicon promoting the formation of an $(Ni)_x(Mo,Cr)_y(C,Si)$ phases rather than true M_6C or $(Mo,Cr)_2C$. At low silicon concentrations, the latter are present, whereas at the high levels found in commercial air-melted material only the pseudocarbides occur. It is only the $(Ni)_x(Mo,Cr)_y(C,Si)$ that transforms to the high-temperature phase.

We have not found any published information suggesting that silicon replaces part of the carbon in the M_6C structure although several researchers have proposed that it occupies metal sites. (7,8) Our findings strongly indicate that the former is actually the case, particularly in view of the observations that the amount of precipitate increases greatly as the silicon content is increased. The behavior of the pseudocarbides is also very dependent on the silicon concentration of the alloy. Class et al. (9) have found that silicon enhances the formation and stability of sigma phase in several Ni-Cr-Mo alloys.

Cracking appears to initiate in weld fusion zones containing the transformed product. As mentioned previously, these areas are enriched in silicon. Thus, the formation of the high-temperature phase is associated with increased embrittlement.

The rupture ductility is quite sensitive to heat treatments which promote the formation of the high-temperature phase. Although the phase is not observed at the lowest annealing temperatures showing low ductility in Fig. 2, it is reasonable that changes are occurring on a microscale which could severely embrittle the material. We have shown that the grain-boundary fracture surface contains massive amounts of precipitate after fracturing a specimen at 870°C subsequent to a 1260°C anneal and that at least one morphology is severely attacked by the 10% HCl–alcohol electrolyte. This attack would not be expected if the phase were a carbide. We also have observed electrolyte attack on the high-temperature phase.

We are not able to propose a specific mechanism to explain the decreased elevated temperature ductility in this very complex alloy but

have found that silicon affects the ductility in a deleterious manner. Several possibilities could be cited to explain this effect but the mechanism is probably a complex combination of several effects. A phase formed at high temperatures present in the grain boundaries is surely a contributing factor to the increased embrittlement. This could be mechanically brittle, affect the grain-boundary surface energy and crack propagation, or the composition of areas adjacent to the boundaries. We have found that cold work following a 1260°C anneal results in recovery of the ductility, which would support any of the above possibilities. We have found that, on testing at 870°C, material annealed at 1180°C has good ductility with a recrystallized microstructure whereas material annealed at 1260°C has very low ductility without any recrystallization (Fig. 4). This would suggest that after the higher temperature anneals, cracks nucleate and grow before normal deformation processes begin, which would result in premature failure without recrystallization, whereas for material annealed at 1180°C the grain boundaries are able to deform to relieve stress concentrations and allow additional matrix deformation to premit recrystallization (see Fig. 4). Impurity effects in or adjacent to grain boundaries after high-temperature anneals may pin the boundaries and prevent their migration. Nevertheless, it is far from clear as to which, if any, of these effects would be predominant.

SUMMARY

We have found that changes in, and behavior of, mechanical properties and precipitates in Hastelloy N can be related to the silicon concentration. In air-melted heats, containing about 0.6% Si, the only precipitates which form at temperatures as high as 1180°C are complex pseudocarbides of the $Ni_3(Mo,Cr)_3(C,Si)$ and $Ni_2(Mo,Cr)_4(C,Si)$ types, the former being large primary particles and the latter resulting from exposure to elevated temperatures in the range 500 to 1000°C. At temperatures in excess of 1300°C, these precipitates transform to a high-temperature phase, possibly the NiMo intermetallic.

In vacuum-melted heats containing low amounts of silicon, the mode of precipitation changes, with M_6C primary carbides and $(Mo,Cr)_2C$ also present. The M_6C in this material is taken into solid solution at high annealing temperatures and the high-temperature phase does not form. The elevated temperature ductility losses are much less severe in the low silicon materials than in the alloys containing higher amounts of silicon. The high-temperature phase is associated with deleterious ductility losses at elevated temperatures.

REFERENCES

1. W. D. Manly et al., Metallurgical Problems in Molten Fluoride Systems, Progr. Nucl. Energy (Ser.IV) 2; Technology, Engineering, and Safety, Pergamon Press, New York, 1960, pp. 164–179.

2. C. K. DuBose and J. O. Stiegler, Semiautomatic Preparation of Specimens for Transmission Electron Microscopy, ORNL-4066, February 1967.

3. H. E. McCoy, Influence of Several Metallurgical Variables on the Tensile Properties of Hastelloy N, ORNL-3661, August 1964.

4. F. N. Rhines and P. J. Wray, Investigation of the Intermediate Temperature Ductility Minimum in Metals, Trans. ASM 54, 117 (1962).

5. P. V. Guthrie and E. E. Stansbury, X-Ray and Metallographic Study of the Nickel-Rich Alloys of the Nickel-Molybdenum System II, ORNL-3078, July 1961, p. 55.

6. C. B. Shoemaker et al., X-Ray Diffraction Studies of the δ Phase, Mo–Ni, Acta Cryst. 13, 585 (1960).

7. M. N. Kozlova and N. F. Lashko, Double Carbides Containing Silicon, J. Inorg. Chem. (USSR) 2(11), 47–50 (1957). Translation.

8. A. Taylor and K. Sachs, A New Complex Eta-Carbide, Nature 169(4297), 411 (1952).

9. I. Class et al., Development of a Corrosion-Resistant Nickel-Chromium-Molybdenum Alloy with Segregation Inertia, Z. Metall. 53(5), 283–293 (1962).

ACKNOWLEDGMENTS

The authors are indebted to many persons for their assistance in this study: J. T. Houston, C. Jones and S. W. Cook, assistance in electron microscopy studies; H. Mateer, R. S. Crouse, T. J. Hinson, and G. Hallerman, electron microprobe analyses; M. D. Allen, autoradiography; H. R. Tinch and G. D. Stohler, metallography; B. C. Williams and P. F. Huber, mechanical testing; R. S. Steele, x-ray diffraction analyses; Metals and Ceramics Division Reports Office and ORNL Graphic Arts Department, preparation of manuscript; and Metals and Ceramics Materials Processing Laboratory, preparation and fabrication of experimental alloys. In addition, the authors are grateful to J. O. Stiegler, H. Inouye, J. R. Weir, Jr., and H. Mateer for their valuable technical suggestions and discussions, and to C. J. McHargue, J. O. Stiegler and C. E. Sessions for reviewing the manuscript.

Table 1. A Comparison of the Specified Chemical Composition of Hastelloy N with that Normally Obtained

Element	Content, wt%[a]		
	Specified	Typical, Air-Melted[b]	Typical, Vacuum-Melted[c]
Ni	Bal		Bal
Mo	15.0–18.0	16.5	17.0
Cr	6.0– 8.0	7.26	6.2
Fe	5.0	3.90	0.03[d]
C	0.04–0.08	0.06	0.056
Mn	1.0	0.55	0.21
Si	1.0	0.60	0.05
W	0.50	0.03	0.01
Al	0.50	0.01	0.15
Ti		0.01	0.067
Cu	0.35	0.01	< 0.01
Co	0.20	0.07	0.04
P	0.015	0.004	0.002
S	0.020	0.007	0.002
B	0.010	0.005	0.0010
O, N		0.013	0.002
Others, total	0.50		

[a] Single values are maximum percentages.

[b] Heat 5065.

[c] Heat 2477.

[d] This element does not seem to be important. It was originally present to allow the chromium to be charged as ferrochrome. The trend in vacuum melting seems to be to not make any intentional iron addition.

Table 2. X-Ray Diffraction Data[a] From Extracted Precipitates

M_6C-type[b] a = 11.01 ± 0.02 Å			$(Mo, Cr)_2C$[c] a = 2.98 Å, c = 4.688 Å		
d	I/I_o	hkl	d	I/I_o	hkl
3.883	1	220	2.578	24	100
3.314	3	331	2.344	40	002
3.175	7	222	2.263	100	101
2.750	7	400	1.734	22	102
2.522	9	331	1.490	18	110
2.246	29	422	1.337	17	103
2.118	100	333/511			
1.945	14	440			
1.834	3	600			
1.731	2	620			
1.661	1	622			
1.541	3	711			
1.435	3	731			

[a] Monochromated CuK_α radiation, scintillation counter, pulse height analyzer, Norelco goniometer.

[b] 2θ range: 20 to 65°. Precipitate is a combination of $(Ni)_x (Mo, Cr)_y (C, Si)$ with x = 3, y = 3 and x = 2, y = 4.

[c] 2θ range: 20 to 75°. Composition is approximately $(Mo_{0.8}Cr_{0.2})_2C$.

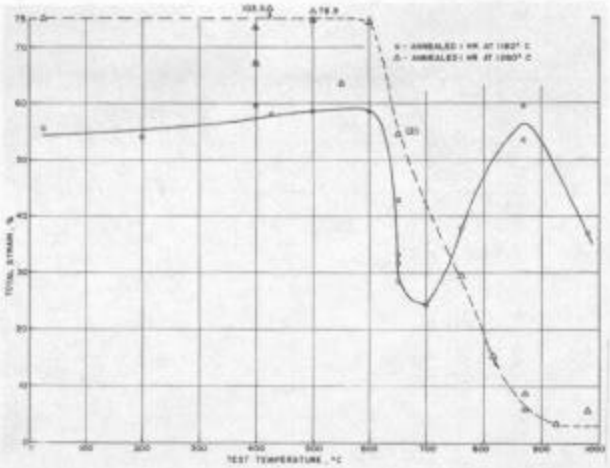

Fig. 1. Effect of test temperature on rupture strain for pretest annealing temperatures of 1180 and 1260°C.

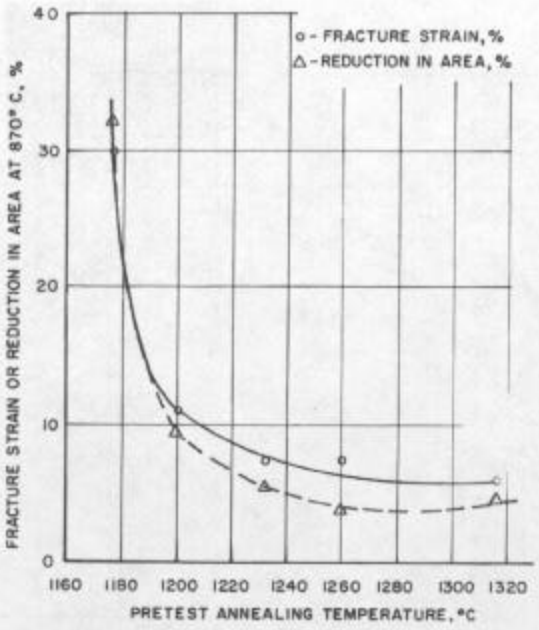

Fig. 2. Effect of pretest annealing temperature on the rupture ductility at 870°C.

Fig. 3. Typical microstructure of wrought Hastelloy N showing the heterogeneous distribution of primary stringered M_6C-type precipitates. Etchant: glyceria regia. 100×.

H-72219

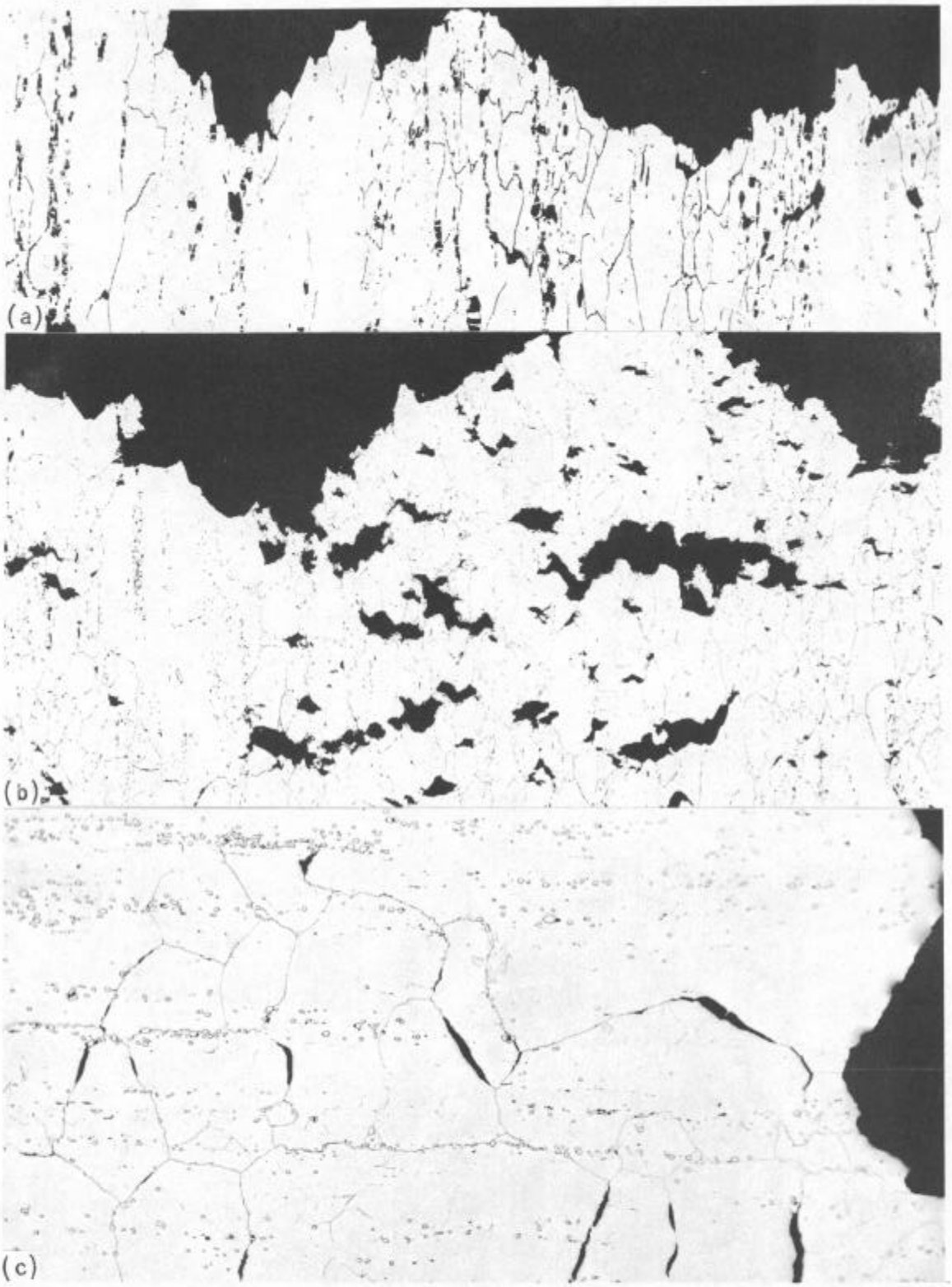

Fig. 4. Microstructure of Hastelloy N specimens fractured at 25°C (a) and 980°C (b,c) following pretest anneals at 1180°C (a,b) and 1260°C (c). Note particle cracking and transgranular separation in (a), intergranular separation and recrystallization in (b), and very little separation or deformation away from fracture and no recrystallization in (c). Etchant: gylceria regia. 100×.

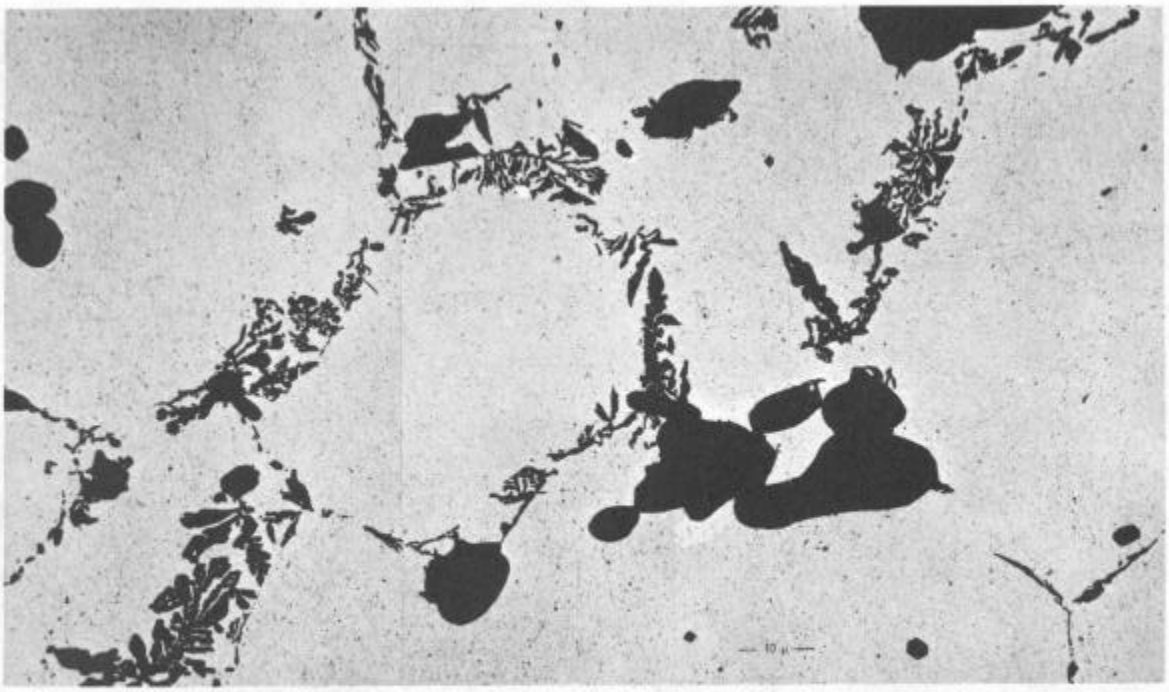

Fig. 5. Direct carbon electrolytic extraction replica from Hastelloy N aged 4 hr at 870°C following an 1180°C anneal. Both primary (stringered) and grain boundary carbide-type precipitates are present. 1000×.

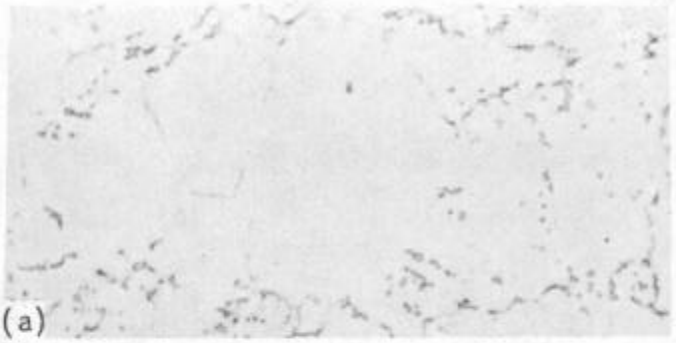

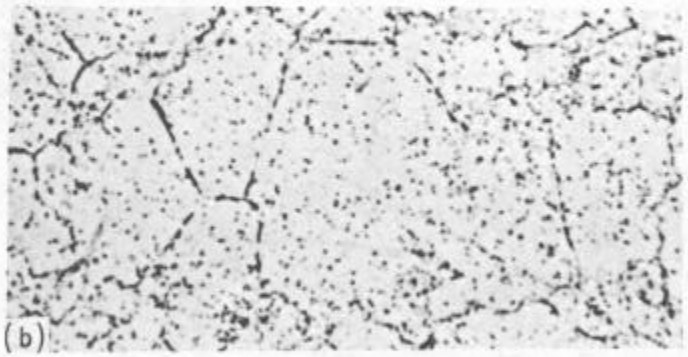

Fig. 6. Carbon-14 doped specimen annealed at 1180°C, aged 100 hr at 650°C, showing activity (dark regions) at precipitates and in grain boundaries. (a) Lightly etched in 10% HCl–alcohol. (b) Same area as (a) but with NTB-2 autoradiographic emulsion exposed 100 hr. 500×.

H-72221

H-72221

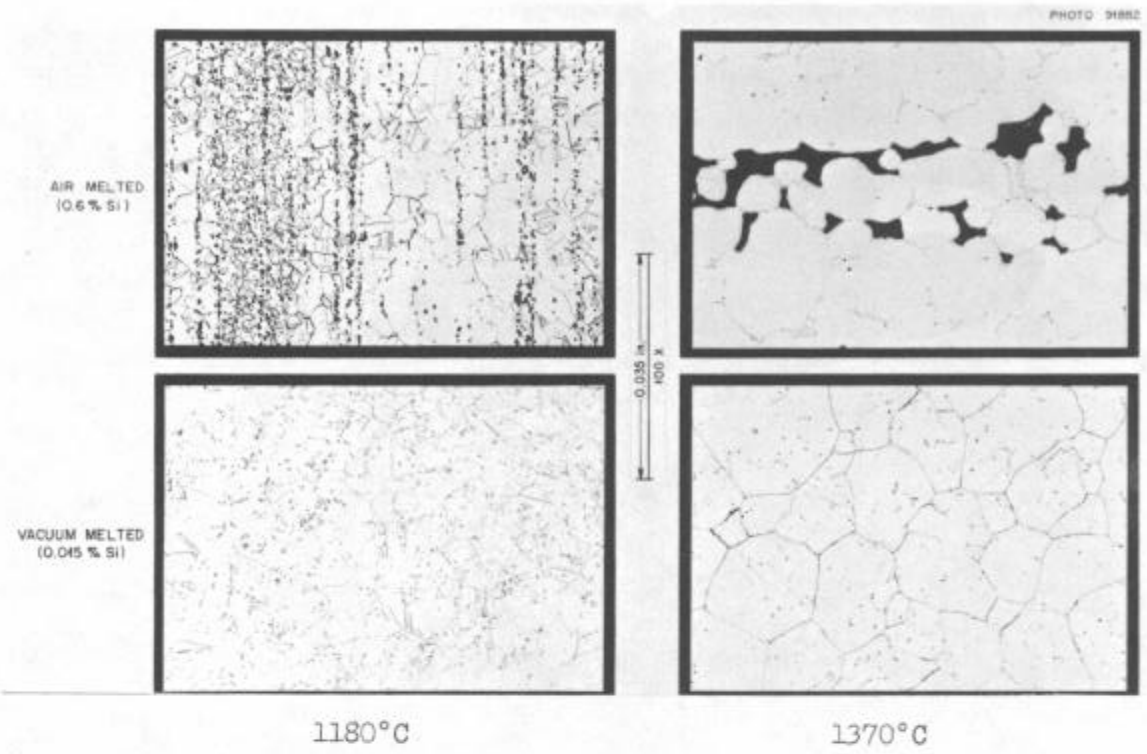

Fig. 7. High-temperature phase transformation occurring in Hastelloy N. Annealed 1 hr at the specified temperatures. 100×. Reduced 62%.

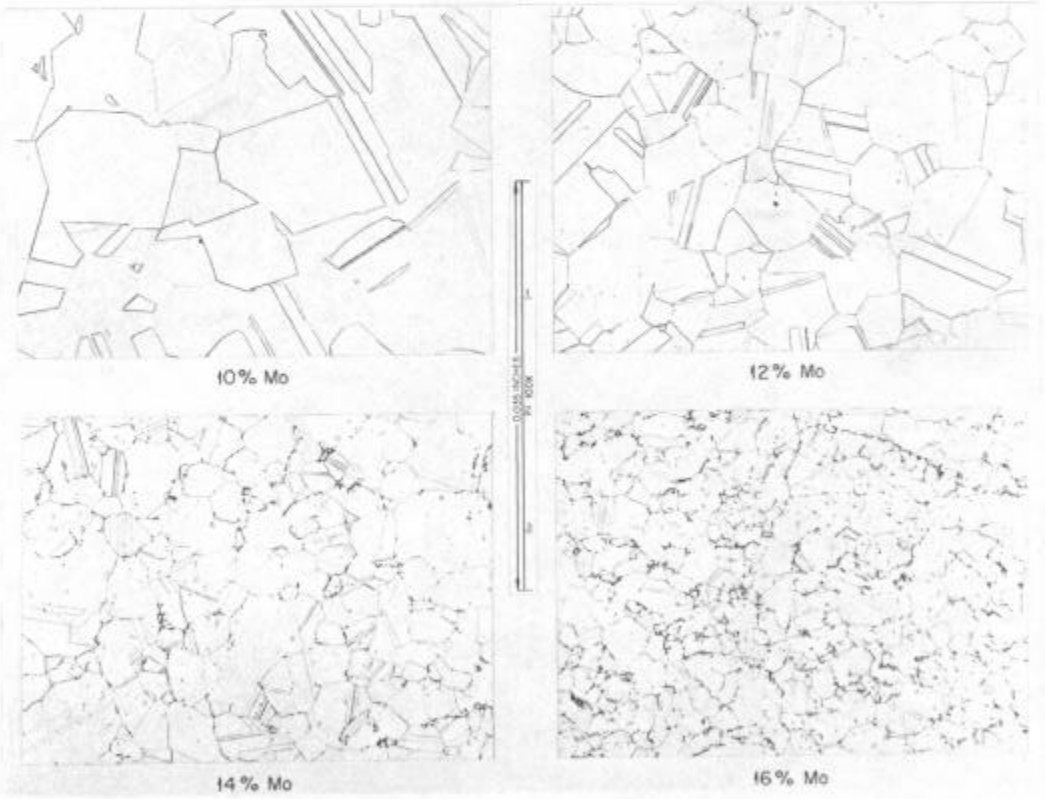

Fig. 8. Effect of molybdenum concentration on precipitation in experimental alloys of Ni–7% Cr–4% Fe–0.2% Mn–0.06% C. Annealed 1 hr at 1180°C. 100×. Reduced 60%.

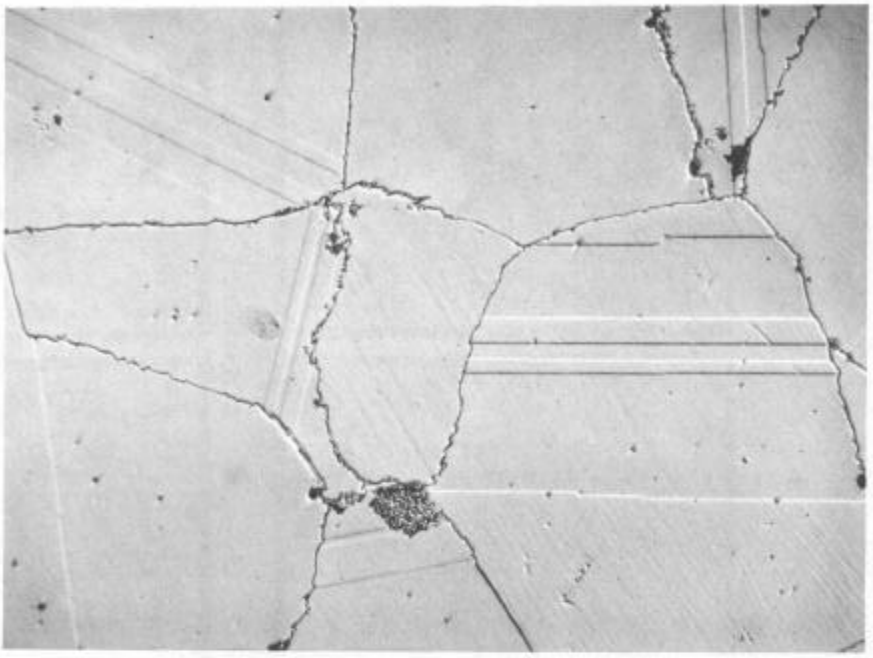

Fig. 9. High-temperature phase in an experimental alloy of Ni–12% Mo–7% Cr–4% Fe–0.5% Mn–0.6% Si–0.05% C. Annealed at 1370°C. Etchant: glyceria regia. 125×.

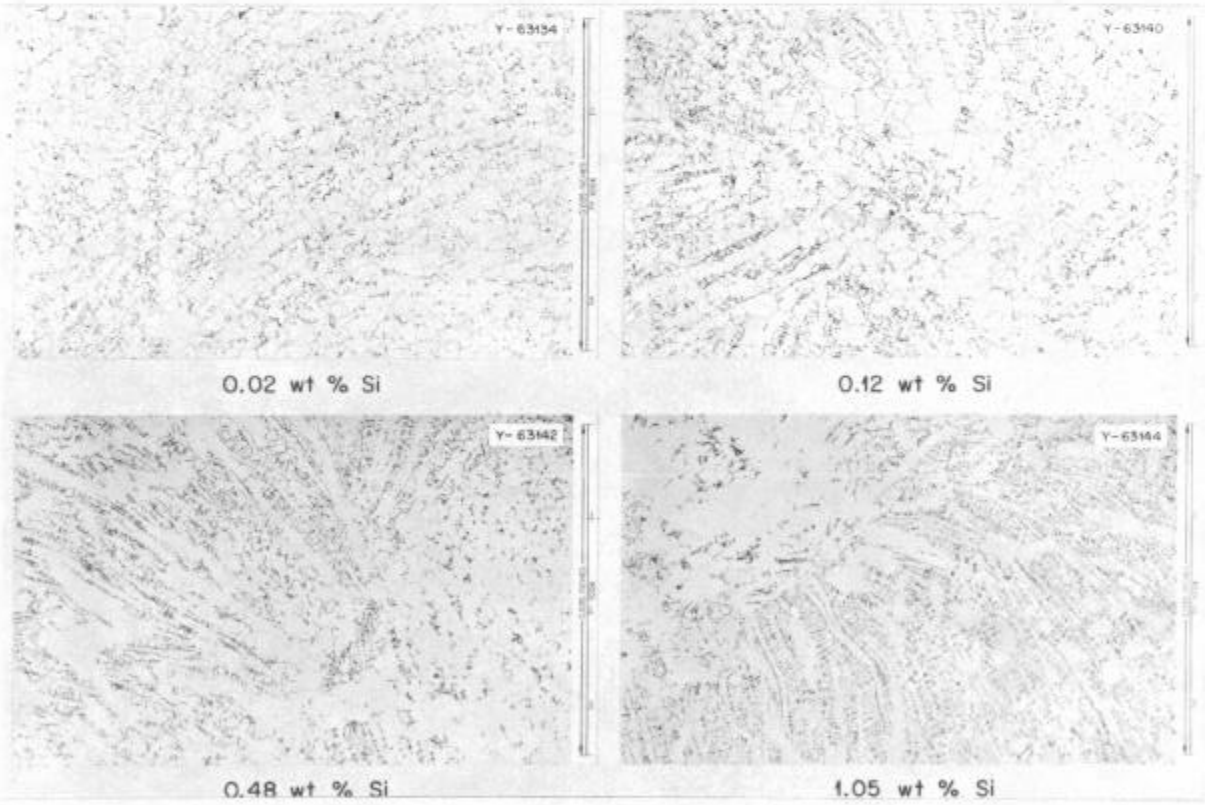

Fig. 10. Effect of silicon concentration on precipitation in experimental alloys of Ni–16% Mo–7% Cr–4% Fe–0.05% C. Annealed 1 hr at 1370°C. Etchant: glyceria regia. 100×. Reduced 53%.

H-72223

H-72223

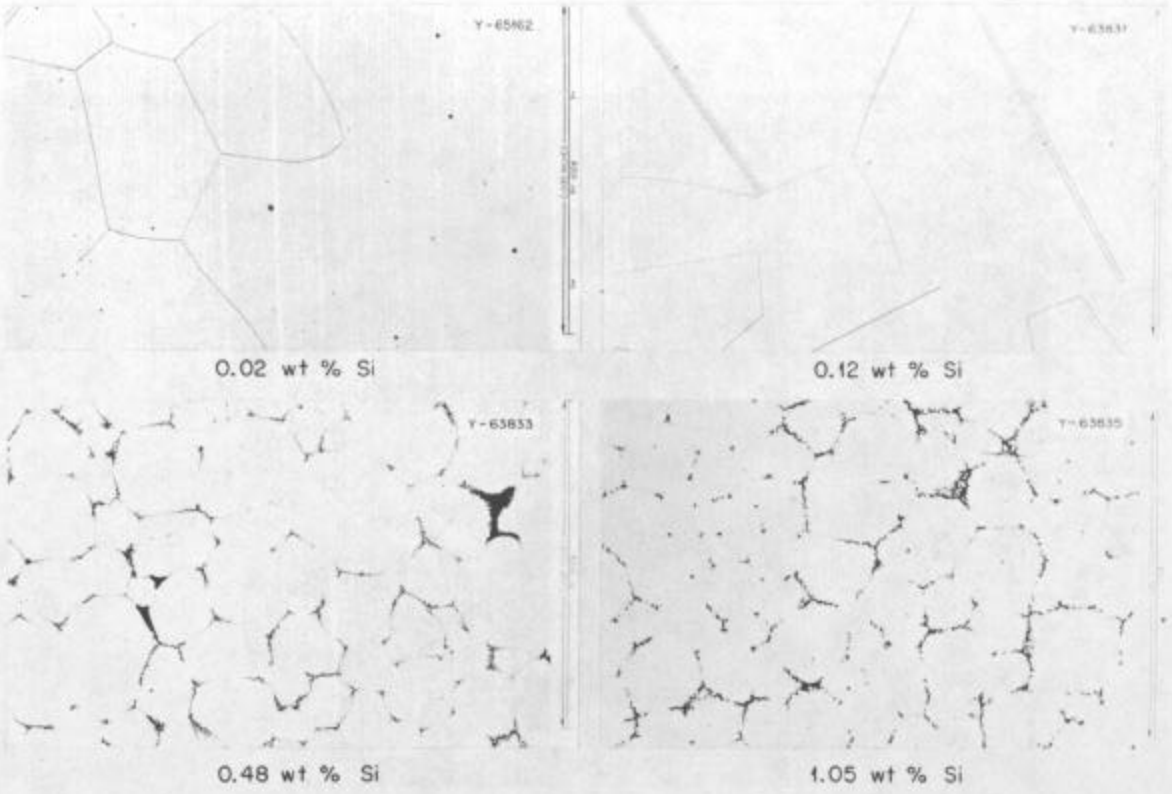

Fig. 11. Effect of silicon concentration on high-temperature phase formation and grain boundary melting in experimental alloys of Ni–16% Mo–7% Cr–4% Fe–0.05% C. Annealed 1 hr at 1180°C. Etchant: glyceria regia. 100×. Reduced 53%.

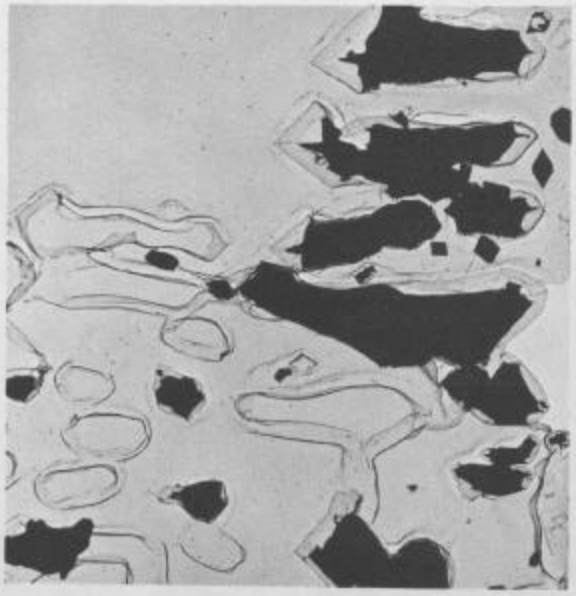

Fig. 12. Direct carbon extraction replica from Hastelloy N annealed 1 hr at 1370°C. The remaining precipitate has an M_6C-type structure with a composition near $Ni_2(Mo,Cr)_4C$ and is enriched in silicon. 6000×.

Fig. 13. Direct carbon extraction replica from the fracture surface of Hastelloy N annealed 1 hr at 1260°C and fractured at 870°C. Note that one thin morphology has reacted with the HCl–alcohol electrolyte. 2500×.

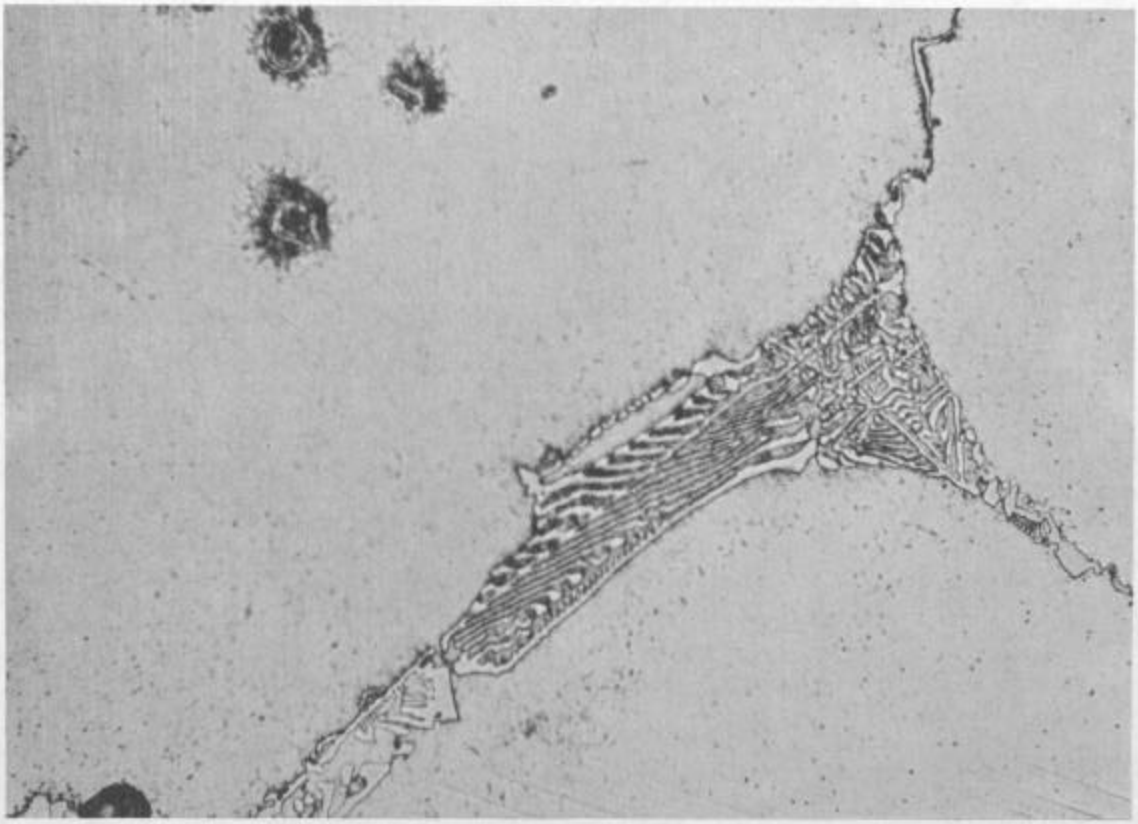

Fig. 14. Autoradiograph of high-temperature phase in carbon-14 doped Hastelloy N. The exposed (dark) areas on the emulsion show that activity emanates from matrix adjacent to the phase, indicating that the phase is not a carbide. NTE emulsion, 312 hr exposure. 1000×.